Supporting information

Delocalized Bi-tetrahedral cluster induced ultralow lattice thermal conductivity in $Bi_3Ir_3O_{11}$

Jialin Ji[1], Zhehong Liu[2,3], Jianhong Dai[2,3], Di Qiu[1,4], Jiong Yang[1,4], Jinyang Xi[1,4,*], Youwen Long[2,3,5,*], and Wenqing Zhang[6,7,*]

[1]Materials Genome Institute, Shanghai University, Shanghai 200444, China.

[2]Beijing National Laboratory for Condensed Matter Physics, Institute of Physics, Chinese Academy of Sciences, Beijing 100190, China.

[3]School of Physical Sciences, University of Chinese Academy of Sciences, Beijing 100049, China.

[4]Zhejiang Laboratory, Hangzhou, Zhejiang 311100, China.

[5]Songshan Lake Materials Laboratory, Dongguan, Guangdong 523808, China.

[6]Department of Materials Science and Engineering and Shenzhen Institute for Quantum Science & Technology, Southern University of Science and Technology, Shenzhen, Guangdong 518055, China.

[7]Shenzhen Municipal Key-Lab for Advanced Quantum Materials and Devices and Guangdong Provincial Key Lab for Computational Science and Materials Design, Southern University of Science and Technology, Shenzhen, Guangdong 518055, China.

Corresponding Authors:

Jinyang Xi, Email: jinyangxi@t.shu.edu.cn

Youwen Long, Email: ywlong@iphy.ac.cn

Wenqing Zhang, Email: zhangwq@sustech.edu.cn

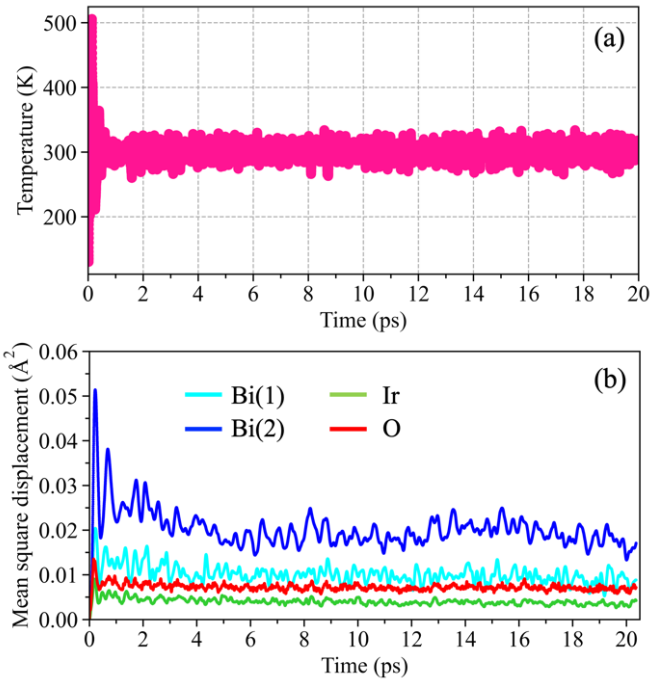

Figure S1. (a) Temperature and (b) average atomic mean square displacements as a function of time from AIMD simulation.

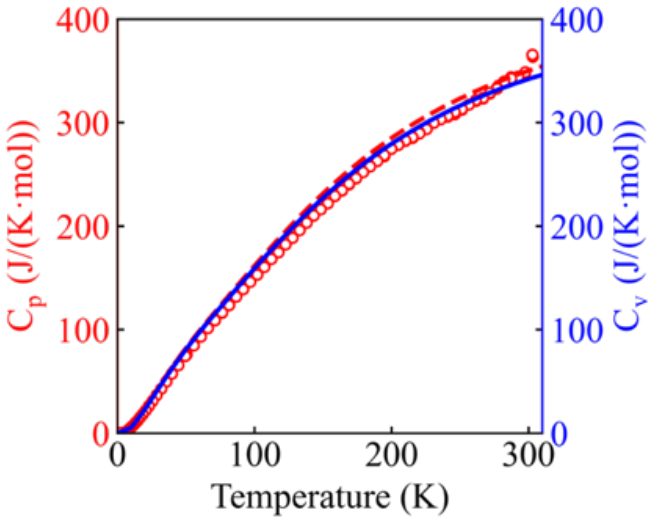

Figure S2. The theoretical and experimental (red hollow circle) values corresponding to heat capacity in $Bi_3Ir_3O_{11}$. The solid blue line is heat capacity at constant volume (C_v) and the dash red line is heat capacity at constant pressure (C_p)

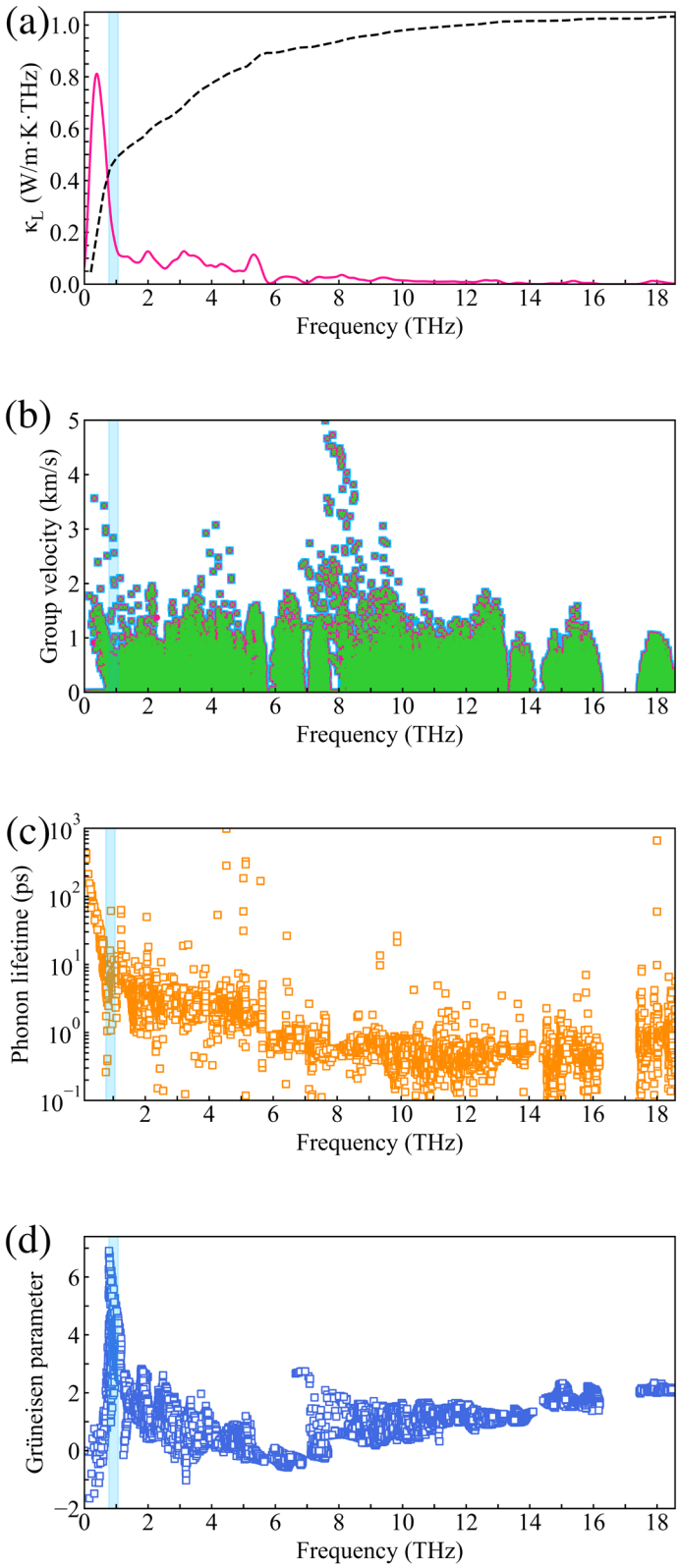

Figure S3. Thermal transport properties as the function of phonon frequency in $Bi_3Ir_3O_{11}$ at 300K. (a) Accumulative lattice thermal conductivity (dash black line) and the spectral lattice thermal conductivity (solid pink line), (b) phonon lifetime, (c)

phonon group velocity and (d) Grüneisen parameter. The blue regions represent the results of frequency at the range of 0.77~1.06 THz.

To check whether the oscillators exist, participation ratio (PR) is adopted to characterize the localization of the phonon mode by the participation degree of all atoms as described by:

$$p(\omega_\lambda) = \left(\sum_i^N \left|\frac{\boldsymbol{e}_i(\omega_\lambda)}{\sqrt{M_i}}\right|^2\right)^2 / N\sum_i^N \left|\frac{\boldsymbol{e}_i(\omega_\lambda)}{\sqrt{M_i}}\right|^4 \quad (2)$$

where $\boldsymbol{e}_i(\omega_{\boldsymbol{\lambda}})/\sqrt{M_i}$ is the displacement amplitudes of the atom i. The PR closing to 1.0 means the propagative phonon modes, like the acoustic branches; the PR around or lower than 0.2 indicates the localization mode where very few atoms have large displacements and other atoms keep still. As shown in Supplementary Figure S5, Bi2 dominant modes are localized since their PR is mainly concentrated on the part lower than 0.2.

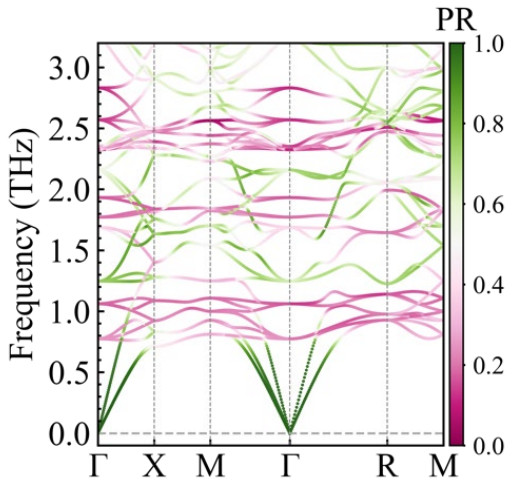

Figure S4. phonon dispersion and the color-coded participation ratio onto the phonon dispersion of $Bi_3Ir_3O_{11}$ at 300K.

Based on IFCs and MD trajectories, the atomic mean square displacements (MSD) are analyzed.

(1). The expectation value of the MSD by IFCs is calculated as[1, 2]

$$\langle|u^\alpha(jl,t)|^2\rangle = \frac{\hbar}{2Nm_j}\sum_{\mathbf{q},v}\ \omega_v(\mathbf{q})^{-1}\big(1+2n_v(\mathbf{q},T)\big)|e_v^\alpha(j,\mathbf{q})|^2 \quad (3)$$

where j and l are the labels for the j-th atomic position in the l-th unit cell, t is the time, α is an axis, m is the atomic mass, N is the number of the unit cells, $\mathbf{q}$ is the wave vector, ν is the index of phonon mode. e is the polarization vector of the atom jl and the band ν at $\mathbf{q}$. $\mathbf{r}(jl)$ is the atomic position and ω is the phonon frequency. $n_\nu(\mathbf{q},T)$ is the phonon population, which is given by

$$n_\nu(\mathbf{q},T) = \frac{1}{\exp\left(\hbar\omega_\nu(\mathbf{q})/k_BT\right)-1} \tag{4}$$

where T is the temperature, and k_B is the Boltzmann constant.

(2). The expectation value of the mean squared atomic displacement by MD trajectories, as described by

$$\mathrm{MSD} \equiv \langle|\mathbf{x}(t)-\mathbf{x}_0|^2\rangle = \frac{1}{N}\sum_{i=1}^{N}\left|\mathbf{x}^{(i)}(t)-\mathbf{x}^{(i)}(0)\right|^2 \tag{5}$$

where N is the number of particles to be average, vector $\mathbf{x}^{(i)}(0)=\mathbf{x}_0^{(i)}$ is reference position of the i-th particle, and vector $\mathbf{x}^{(i)}(t)$ is the position of the i-th particle at time t[3] . It needs to be noted that $\langle|u^\alpha(jl,t)|^2\rangle$ and MSD are of the same meaning but in different expressions.

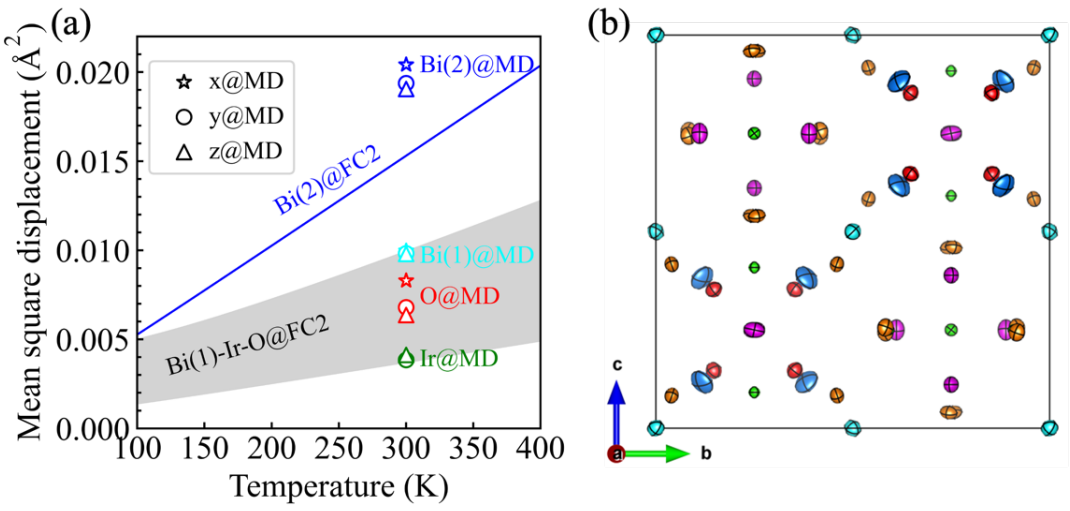

Figure S5. Mean square displacements (MSD) and mean square displacement matrix of $Bi_3Ir_3O_{11}$. (a) MSD of each atom is calculated from harmonic IFCs (lines and grey regions) and MD trajectory (hollow symbol) at 300K. (b) MSD matrix. Color of atoms are the same of Figure 1.

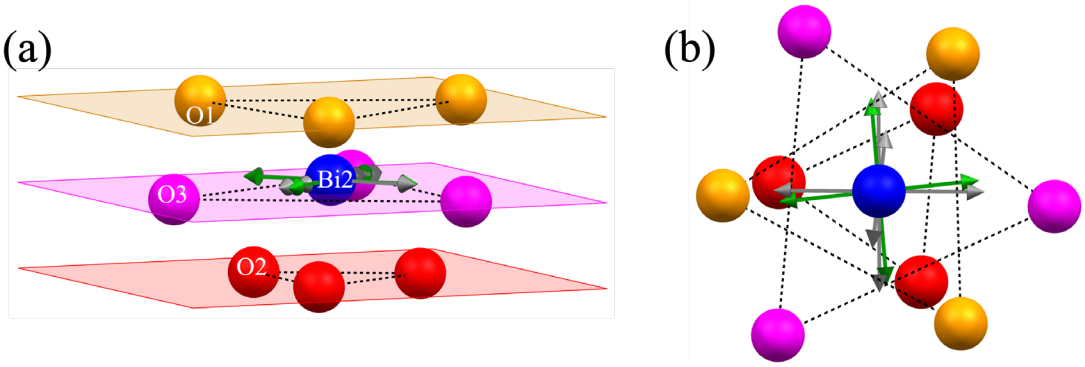

Figure S6. (a). Side view, and (b) top view of schematic of the atomic vibration of Bi2. The parallelogram indicates the plane of oxygen near the Bi2. The plane formed by $O2_3$ is parallel to $O1_3$ and $O3_3$. The arrows on the Bi2 represent the vibrational directions of low-frequency optical modes (0.77 and 1.06 THz) at Γ point. The Bi2 vibrates in parallel with these oxygen planes.

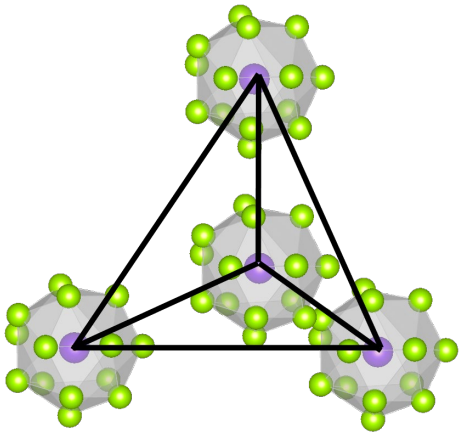

Figure S7. Schematic of the delocalized cluster. The purple atom is a ratter in a large cage (green atoms). Four purple atoms form a delocalized cluster with large mean square displacement and “large atomic mass”.

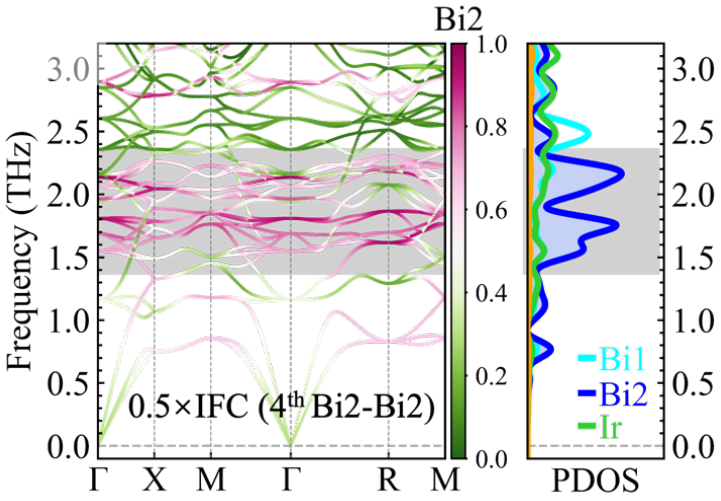

Figure S8. Phonon dispersion and the density of states of Bi2 atoms projects onto the phonon dispersion are also shown and phonon PDOS in the toy model (reducing the 4th neighboring Bi2-Bi2 interaction to half of the actual interaction). The grey regions represent frequency of main contribution for Bi2 atoms.

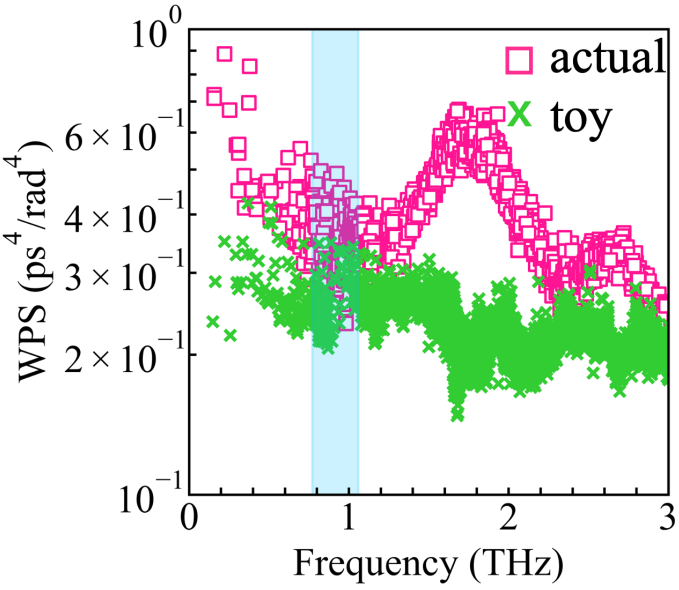

Figure S9. The weighted scattering phase space (WPS) of actual (pink color) and toy models (green color) in $Bi_3Ir_3O_{11}$ at 300 K, respectively. The low-lying optical phonons range (0.77~1.06 THz) is represented in blue.

The mode Grüneisen parameter $\gamma(\mathbf{q}\nu)$ at the wave vector $\mathbf{q}$ and band index ν is given by:

$$\gamma(\mathbf{q}\nu) = -\frac{V}{\omega(\mathbf{q}\nu)}\frac{\partial\omega(\mathbf{q}\nu)}{\partial V} \quad (1)$$

Where V is the volume, and $\omega(\mathbf{q}\nu)$ is the phonon frequency. To calculate phonon-resolved Grüneisen parameters, the equilibrium volumes of $Bi_3Ir_3O_{11}$ are expanded and compressed by 2% to obtain the phonon frequency shifts. Here, we calculated phonon-resolved Grüneisen parameters by phonopy[1]. The phonon-resolved Grüneisen parameters have the same tendency with the Grüneisen parameters derived from the 3rd-order IFCs, but are slightly larger than Grüneisen parameters derived from the 3rd-order IFCs.

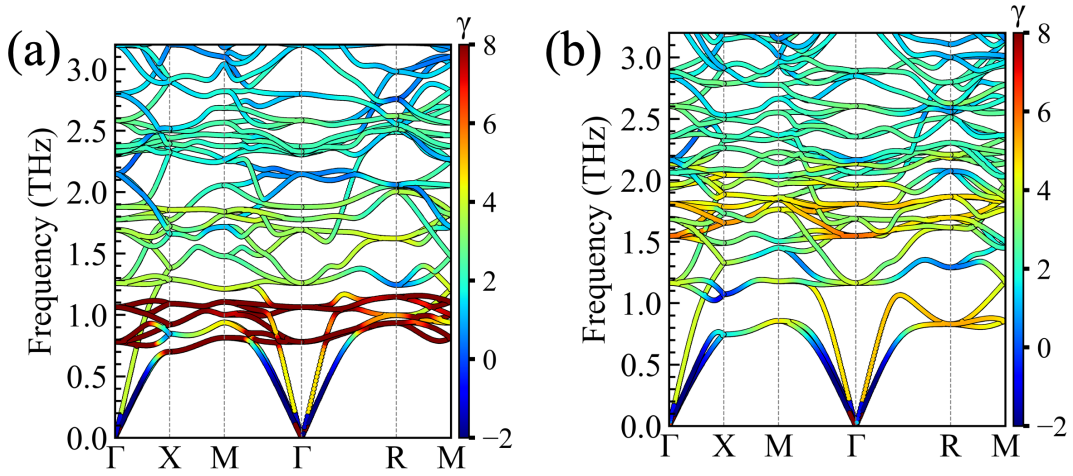

Figure S10. The color-coded mode Grüneisen parameters (γ) are projected onto the phonon dispersion of $Bi_3Ir_3O_{11}$. (a) Actual phonon dispersion, and (b) toy phonon dispersion when reducing the strength of the 2nd IFCs of 4th-neighbor Bi2-Bi2 bonds.

The valence electron configuration of Bi is $6s^26p^3$. Thus, the formally trivalent Bi in most oxides contains a lone pair of 6s electrons, which tend to hybridize with the O 2p orbital, such as $BiMnO_3$[3], Bi_4MO_8X (M = Nb, Ta; X = Cl, Br)[4], and Ba_2BiMO_6 (M = Bi, Nb, Ta)[5]. However, the difference from the above compounds is that the

lone pair of trivalent Bi2 in $Bi_3Ir_3O_{11}$ may arise from sp^3 hybridization. There are two main reasons to support our point of view:

(i). Figure S11 depicts the electronic projected density of states, and the partial charge density for various energy regions. Among the b-e regions, only the d region has the lone pair character with the red semilunar, whose character is similar to Figure 5. Then, we focus on the d region and divide it into two parts, the f region (yellow color) and the g region (cyan color). As shown in Figures S11f and S11g, the f region presents the distinguishing feature of lone pairs. Thus, the electron states lying in the f region correspond to the lone pair of Bi2. Furthermore, in Figure S11a, the ratio of the s orbital area to the p orbital area in the f region is close to 1:3. As a result, it indicates that the lone pair of trivalent Bi2 in $Bi_3Ir_3O_{11}$ arises from the sp^3 hybridization.

(ii). As shown in the Figure 4 of the revised manuscript, there is a delocalized strong interaction in $Bi2_4$. Thus, the four Bi2 atoms can be regarded as forming a tetrahedral cluster. In the previous study of tetrahedral P_4 (white phosphorus), each P atom is in a state of sp^3 hybrid orbital, three orbitals take part in the formation of P-P bonds (bent electron pair bonds outside the edges, called bent bond or banana bond), and the other one is the lone pair of electrons (Figure S12)[6, 7]. Tetrahedral molecules, such as As_4, Sb_4, and Bi_4, also have similar configurations[8]. Thus, it is reasonable that the trivalent Bi in the tetrahedral $Bi2_4$ of $Bi_3Ir_3O_{11}$ has sp^3 hybridized lone electron pairs.

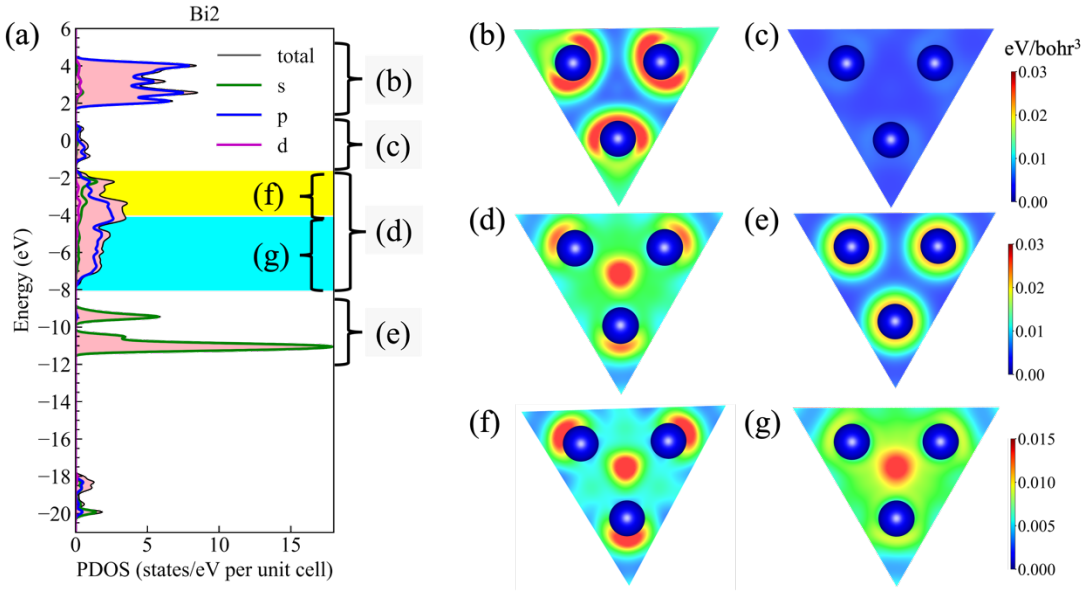

Figure S11. (a) Electronic projected density of states in $Bi_3Ir_3O_{11}$. (b-g) Partial charge density (band decomposed charge density). These correspond to the six energy regions shown with brackets in (a). In particular, the d region in (a) is divided into two parts, f region (yellow color) and g region (cyan color), respectively.

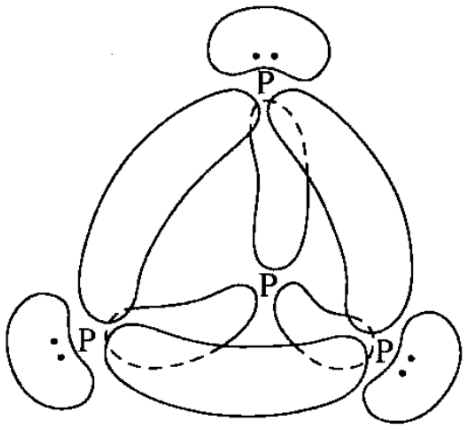

Figure S12. The schematic of the geometric structure and the electron density of tetrahedral P_4 molecular [8].

References:

1. Atsushi Togo and Isao Tanaka, First principles phonon calculations in materials science, Scripta Materialia 108 (2015): 1-5.

2. Alexandra Navrotsky, Thermodynamics of Crystals, Eos Transactions American Geophysical Union 80(13) (2013): 143-143.

3. Ram Seshadri and Nicola A. Hill, Visualizing the Role of Bi 6s "Lone Pairs" in the Off-Center Distortion in Ferromagnetic $BiMnO_3$, Chemistry of Materials 13(9) (2001): 2892-2899.

4. Hironobu Kunioku, Masanobu Higashi, Osamu Tomita, Masayoshi Yabuuchi, Daichi Kato, Hironori Fujito, Hiroshi Kageyama, and Ryu Abe, Strong hybridization between Bi-6s and O-2p orbitals in Sillén–Aurivillius perovskite Bi_4MO_8X (M = Nb, Ta; X = Cl, Br), visible light photocatalysts enabling stable water oxidation, Journal of Materials Chemistry A 6(7) (2018): 3100-3107.

5. Jueli Shi, Ethan A. Rubinstein, Weiwei Li, Jiaye Zhang, Ye Yang, Tien-Lin Lee, Changdong Qin, Pengfei Yan, Judith L. MacManus-Driscoll, David O. Scanlon, and Kelvin H.L. Zhang, Modulation of the Bi^{3+} $6s^2$ Lone Pair State in Perovskites for High-Mobility p-Type Oxide Semiconductors, Advanced Science 9(6) (2022): 2104141.

6. OLLE MÂRTENSSON and GUNNAR SPERBER, Some Remarks on Charge Densities in Bent Bond Molecules, Acta Chem. Scand 24(5) (1970).

7. A. S Rodin, A. Carvalho, and A. H Castro Neto, Strain-Induced Gap Modification in Black Phosphorus, Physical Review Letters 112(17) (2014): 176801.

8. Gongdu Zhou, Chemistry polyhedron (Chinese Edition), Peking University Press Pub (2009).